European Commission

JRC TECHNICAL REPORTS

Adaptive nitrogen to phosphate ratio in biogeochemical models, consequences for the stoichiometry of the Mediterranean Sea

Macias, Diego; Stips, Adolf; Garcia-Gorriz, Elisa

2018

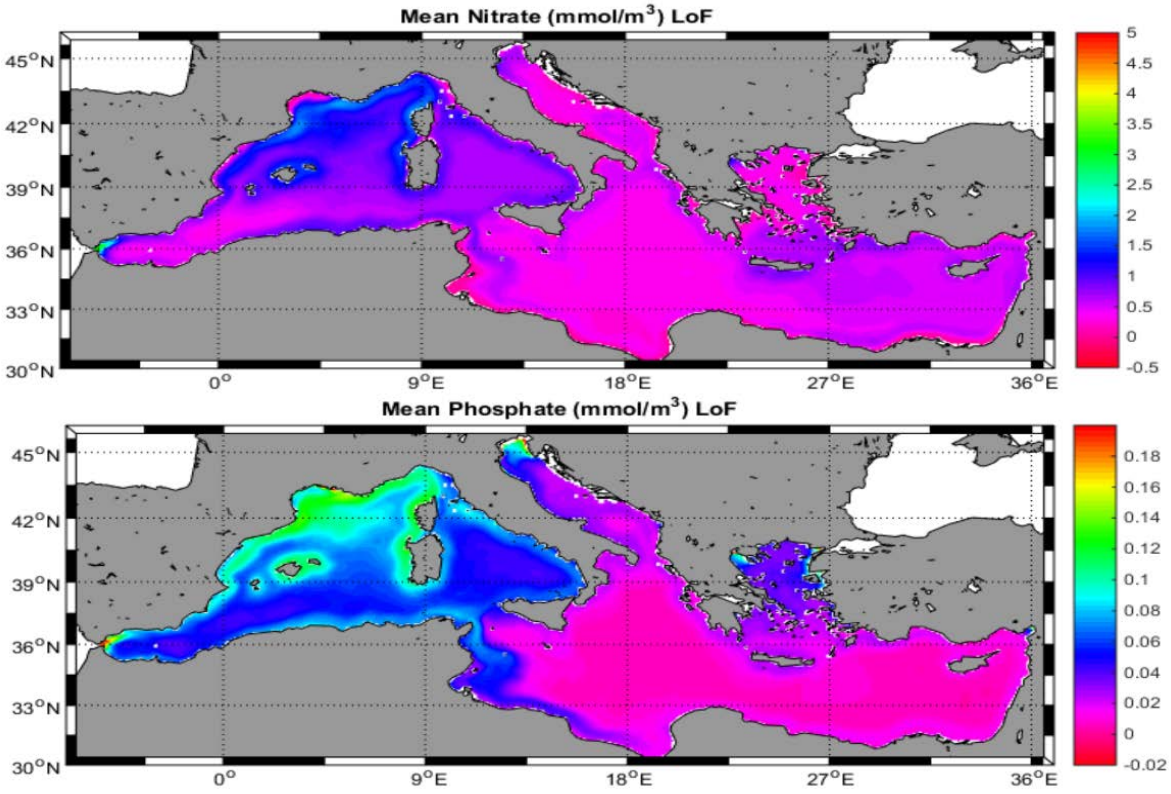

EUR 29142 EN

Contact information
Name: Diego Manuel Macias Moy
Address: Via E. Fermi, TP-270, 21021-Ispra, Varese, Italy
Email: diego.macias-moy@ec.europa.eu
Tel.: +39 0332 789636

JRC Science Hub
https://ec.europa.eu/jrc

JRC111042

EUR 29142 EN

PDF ISBN 978-92-79-80956-9 ISSN 1831-9424 doi:10.2760/797879

Luxembourg: Publications Office of the European Union, 2018

How to cite this report: Diego Macias, Adolf Stips, Elisa Garcia-Gorriz, *Adaptive nitrogen to phosphate ratio in biogeochemical models, consequences for the stoichiometry of the Mediterranean Sea*, EUR 29142 EN, Publications Office of the European Union, Luxembourg, 2018, ISBN 978-92-79-80956-9, doi:10.2760/797879, JRC111042.

Contents

Abstract

Biogeochemical marine models aim to replicate the chemical and low-trophic levels conditions of marine ecosystems. There are many types of such models, depending on complexity, specific aims and formulations. All of them are but rough approximation of the real ecosystems with many shortcomings and drawbacks so improvements and new formulations are always needed in order to increase their capability to reproduce real-life conditions.

Here we present a modification of the biogeochemical model developed at JRC for representing marine conditions in the Mediterranean Sea, the MedERGOM model. This model has been demonstrated to properly represent biological production patterns in the basin but had some difficulties in simulating correctly concentrations of free nutrients in the seawater.

In the present report we modify the internal ratio of the two main nutrients in the sea (nitrate and phosphate) by taking into account the physiological flexibility plankton communities show in the real environment. By making this simple modification we show how nutrients levels in seawater simulated by MedERGOM become much closer to observations, enhancing the capability of the marine modelling framework to simulate chemical conditions in nutrient-starved basins such as the Mediterranean Sea.

1 Introduction

Nutrients are the necessary building blocks for primary producers to create organic matter (OM) through photosynthesis. These are essential chemical elements that are fundamental parts of key molecules within the cells such as the nucleic acid (e.g., phosphorus) or aminoacids and proteins (the case of nitrogen).

In the ocean, the molar ratio of nitrogen to phosphorus (N:P) has been used to determine which of these two 'macro-nutrients' limits phytoplankton production. In the seminal work by A. Redfield (Redfield, 1934) a quasi-constant molar N:P ratio of 16:1 was described for both the seawater ($N:P_{water}$) and for the phytoplankton biomass ($N:P_{OM}$). In Redfield's original work the reasons behind this 'fixed' ration were proposed to be related with '*the characteristic of protoplasm in general*'. Later works have proposed that the $N:P_{OM}$ value is determined by the interdependence of two universal life processes: the syntheses of rRNA and proteins (e.g., Falkowski, 2000; Geider & La Roche, 2002; Sterner & Elser, 2002; Elser et al., 2003; Klausmeier et al., 2004). Loaladze & Elser (2011) described that '*under optimal conditions and based on the best available data for key model parameters, this ratio also quantitatively corresponds to the canonical N:P value of 16*'.

Henceforth, for determining which nutrient is limiting production typically the actual concentration in the seawater is compared with the Redfield ratio (RfR); if the $N:P_{water}$ is above RfR phosphate is considered to be limiting production. If, on the contrary, $N:P_{water}$ is below RfR, nitrate is limiting. This simple approach based on a unique, unspecific threshold value is typically used in biogeochemical models with low complexity (such as those used in global-scale applications) as it saves computational time by not needing to simulate the metabolic routes of each nutrient separately.

However, there is no compelling reason for the specific value of the RfR (Geider & La Roche, 2002; Klausmeier et al., 2004) and there is growing evidence that both $N:P_{water}$ and $N:P_{OM}$ vary regionally throughout the world's ocean (Karpinets et al. 2006; Fransner et al., 2018). Physiological plasticity of cells and assemblages composition changes (Geider & La Roche, 2002) could help to explain the diversity of ratios found in natural waters.

Thus, using a fixed $N:P_{OM}$ ratio in biogeochemical model is not a fully justifiable assumption (e.g., Flynn et al., 2010) specially in marginal seas where nutrients scarcity and/or unbalanced supply from external sources creates very particular chemical environments (Fransner et al., 2018). In these areas, models needs to be able to deal with shifts between phosphorous and nitrogen limitations, changing nutrients loads (from ultra-oligotrophic to eutrophic waters) and physico-chemical gradients such as in the vicinity of rivers' plumes (Baretta-Bekker et al., 1995; Bauer et al., 2013; Blackford et al., 2004).

The variability on internal nutrient ratios could be considered in biogeochemical models by adding separate metabolic routes for each individual nutrient and simulating each pathway independently. This is the method followed by high-complex, plankton-functional-types (PFT) models such as ERSEM (Baretta et al., 1995) and BFM (Vichi et al., 2007). However, this approach increases largely the number of free parameters of the model (which are typically difficult to estimate) and the computational time for model integration. These drawbacks led to PFTs model not being much used in large-areas, 3D ocean circulation applications with some notable exceptions (e.g., Baretta-Bekker et al., 1995; Tagliabue & Arrigo, 2005; Vichi et al., 2007; Ayata et al., 2014).

A recent paper (Galbraith & Martiny, 2015) (G-M15 from now onwards), presented an analysis of the global relationships between chemical conditions in water (nutrients concentrations) and the value of the $N:P_{OM}$ in such environments. Briefly, they found out that the N:C and the P:C relative ratios of the marine organic matter were dependent on the individual nutrient concentration (N or P) in the water. The N:C vs N relationship is quite stable, with the ratio value only changing slightly at very low N concentrations. The

P:C vs P function is, however, very dynamic in the entire range of typical P concentrations. The higher the P, the larger amount of P per C unit is found in the marine OM, this relationship being called Line of Frugality (LoF) by the authors. So, according to G-M15 results, the plankton plasticity for N is much lower than for P (DeVries & Deutsch, 2014) the reason being the different organic compounds both nutrients are involved with (Geider & LaRoche, 2002).

Combining the N:C vs N and the P:C vs P values, G-M15 created a global map of $N:P_{OM}$ based on reported values of N and P concentration in surface waters. This map shows that large deviations from 16:1 (i.e. RfR) are expected in many oceanic regions such as the central anticlyconic gyres and marginal seas (where the ratio is >16) and around polar areas (both Arctic and Antarctic where the ratio is <16). In this same map an already well known characteristic of the Mediterranean Sea could be seen, that is its $N:P_{OM}$ ratio is well above the RfR value (e.g., Tanaka et al., 2011) as also happens on other oligotrophic regions where plankton has to relay on N-rich proteins for gathering scarce resources (Sterner & Elser, 2002).

High $N:P_{OM}$ ratio in the Mediterranean Sea is concomitant to unusually high $N:P_{water}$ in the basin (e.g., Krom et al., 1991). The reasons for this large $N:P_{water}$ in the Mediterranean Sea are not well identified yet as there are two contrasting hypothesis. The first one refers to relatively high nitrogen fixation rates in the basin due to seagrasses and to the activity of N-fixing phytoplankton (e.g., Béthoux et al., 1992, 1998, 2002; Sarmiento et al., 1988; Gruber & Sarmiento, 1997; Pantoja et al., 2002; Ribera d'Alcala et al., 2003). The second hypothesis makes reference to the unbalanced nutrient ratios (N:P higher than normal) in all external nutrient sources to the Mediterranean (Krom et al., 2004 & 2010).

Independently of the reasons, it is clear that assuming RfR in biogeochemical models applied to the Mediterranean basin seems not to be the optimal approach (e.g., Richon et al., 2018). The recently reported LoF relationship (G-M15) opens up a new possibility to use a simpler, low complexity biogeochemical model but still considering the observed existing plasticity in marine ecosystems regarding nutrients dynamics and internal ratios.

Thus, in the present contribution we modify one of the already existing, low-complexity biogeochemical models specifically developed to represent the Mediterranean Sea ecosystem, the MedERGOM model (Macias et al., 2014a) to consider the variable $N:P_{OM}$ ratio following the LoF concept presented by G-M15. We will compare the results of MedERGOM simulations with a constant RfR ratio and the variable LoF version for a common 7 years period (2001 to 2007) exploring changes in nutrients concentrations and ratios both in the horizontal and in the vertical dimensions.

2 Material and methods

Here we use an integrated modelling framework (MMF) developed at the JRC - Ispra of the European Commission to specifically assess the consequences of different scenarios on the ecosystem status of regional European Seas (Stips et al. 2015). This MMF includes the main elements of a Regional Earth System Model (RESM), i.e., the atmosphere, the hydrological basins and the oceans (Fig. 1). The oceanic component of the MMF is composed by two coupled models, a hydrodynamic model based on GETM (Burchard & Bolding, 2002) and a biogeochemical model based on ERGOM (Neumann, 2000).

Figure 1. Simplified diagram of the Marine Modelling Framework (MMF)

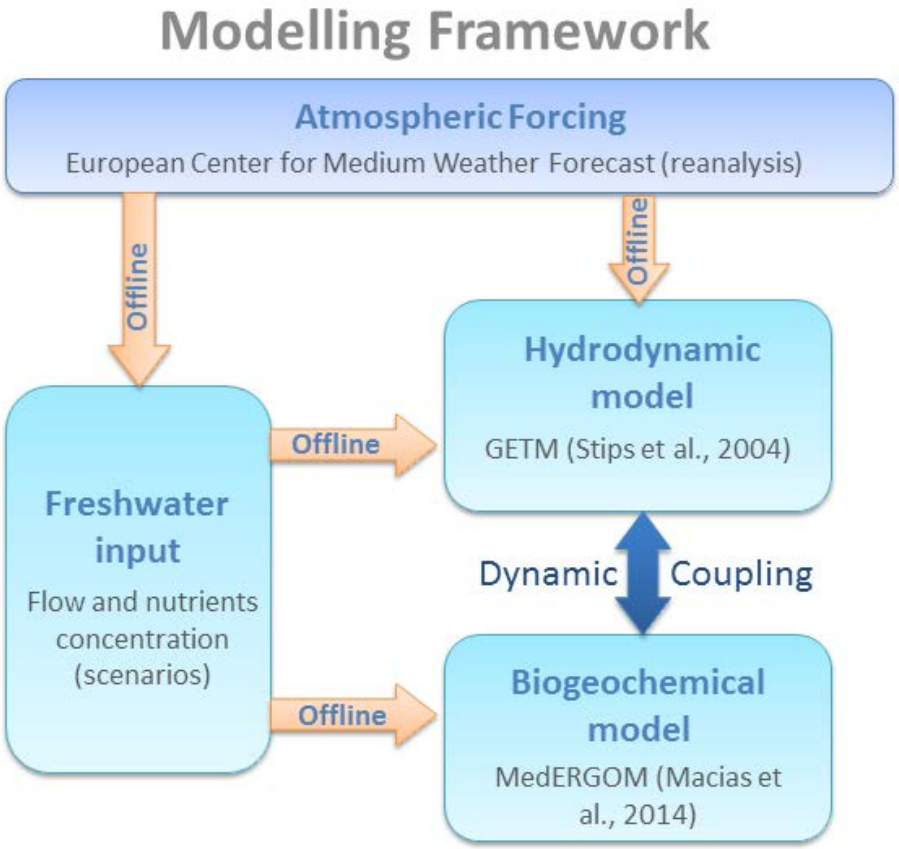

A detailed description of the GETM equations could be found in Stips et al. (2004) and at http://www.getm.eu. Our implementation for the Mediterranean Sea (Fig. 2) has a horizontal resolution of 5' x 5' (~9x9km) and includes 25 vertical sigma-layers. Model bathymetry was built using ETOPO1 (http://www.ngdc.noaa.gov/mgg/global/) database while initial thermohaline conditions were created by using the Mediterranean Data Archeology and Rescue-MEDAR/MEDATLAS database (http://www.ifremer.fr/medar/). The same MEDAR/MEDATLAS data was used to create the boundary conditions for the model at the Strait of Gibraltar where monthly climatological vertically-explicit values of salinity and temperature are imposed. No horizontal currents are explicitly prescribed at the open boundary.

Figure 2. Model domain with bathymetric lines (background colour) and the position of the 53 rivers along the coast (red stars)

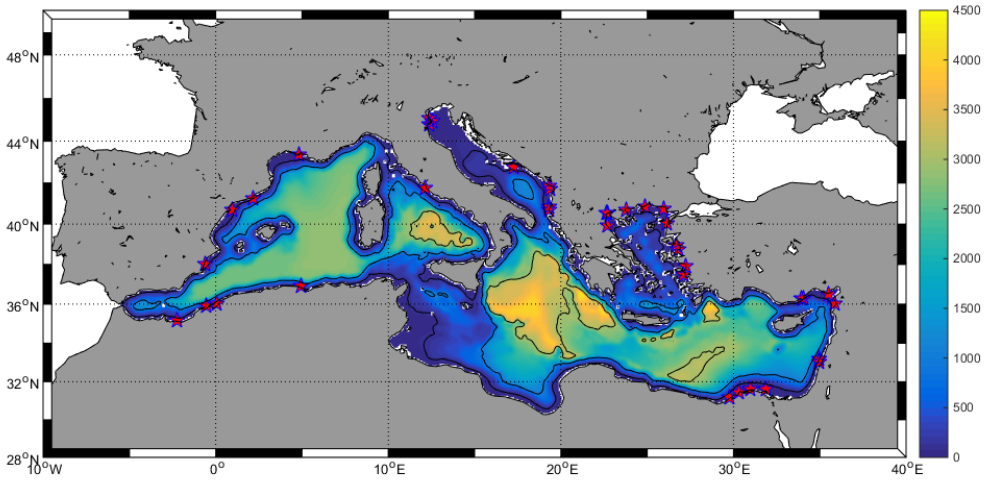

GETM is forced at the surface every 6 hours by the following atmospheric variables: wind velocity at 10 meters, air temperature at 2 m, dewpoint temperature at 2 m, cloud cover and atmospheric pressure at sea level. Atmospheric data comes from the European Centre for Medium-Range Weather Forecasts (ECMWF ERAin database). Bulk formulae are used to calculate the corresponding relevant heat, mass and momentum fluxes between atmosphere and ocean (Macias et al., 2013).

The present configuration of the ocean model includes 53 rivers discharging along the Mediterranean coast (red stars in Fig 2). River inflow is treated as a boundary condition regarding water flow, temperature, salinity and nutrients (computed from the databases mentioned below) with respect to the grid cells where the river is entering. Once in the oceanic domain, the freshwater plume is subjected to the general hydrodynamic processes governing the water movements. Values for river discharges were derived from the Global River Data Centre (GRDC, Germany) database while inorganic nutrient loads (nitrate and phosphate) of freshwater runoff were obtained from Ludwig et al. (2009) who combined literature reports with the Waterbase database at the European Environmental Agency (EAA) to get the most comprehensive, monthly-varying dataset on freshwater quality throughout Europe.

GETM is coupled online to the MedERGOM biogeochemical model (Macias et al., 2014a and 2014b) by using the Framework for Aquatic Biogeochemical Models (FABM, https://sourceforge.net/projects/fabm/, Brueggeman & Bolding, 2014). MedERGOM is a modified version of the ERGOM model (Neumann, 2000) specifically adapted to represent the conditions of the pelagic ecosystem of the Mediterranean Sea. Briefly, MedERGOM incorporates three phytoplankton functional types (‘diatom-like’, ’flagellates-like’ and ‘cyanobacteria-like’), two major nutrients (nitrate and phosphate), one zooplankton compartment and detritus. To get a more comprehensive description of this model the reader is referred to Macias et al. (2014a) and Macias et al. (2017). Biogeochemical initial and boundary conditions are computed from the World Ocean Atlas database (www.nodc.noaa.gov/OC5/indprod.html).

2.1 Nutrients’ incorporation dynamics

The main objective of the present contribution is to compare two different formulations for the nutrient incorporation dynamics in MedERGOM. The equations for nutrients limitation in the model are:

$$nlim = \frac{(NH_4 + NO_3)^2}{\alpha^2 + (NH_4 + NO_3)^2}$$; Eq. 1

$$plim = \frac{{PO_3}^2}{rfr^2 * \alpha^2 + {PO_3}^2}$$; Eq. 2

Being NH_4 the concentration of ammonia in water; NO_3 the concentration of nitrate in water; PO_3 the concentration of phosphate in water; α the half saturation constant (specific for each phytoplankton type) and rfr the P:N ratio in the organic matter. *nlim* stands for 'nitrate limitation' while *plim* stands for 'phosphate limitation'. In MedERGOM (as in ERGOM) the values of *nlim* and *plim* are computed for each position/time-step (ranging 0 -1) and the lowest one is selected as the nutrient-limiting factor.

In the original MedERGOM implementation rfr is set constant at a value of 1:16 (i.e. the Redfield ratio). This value implies that the molar composition of the organic matter (OM) in the original formulation is always 16N to 1P and that the limiting nutrient is defined by the same ratio; if the water concentration is above 16N:1P, phosphate will limit production; if the water concentration is below 16N:1P, nitrogen will be limiting. This is common approach to simulate the co-limitation by different nutrients in low-complexity biogeochemical models that circumvent the need to fully consider the elementary composition of the OM and the different metabolic routes involved. It has, however, the disadvantage of being totally inflexible, not allowing for any physiological and/or community composition changes as response of a change in the chemical conditions of the environmental waters.

In the LoF version of the model we assume that the rfr parameter is variable depending on the concentration of PO_3 in the water. The exact formulation (Eq. 3 below) has been derived from the N:C and P:C relationships provided by G-M15 and assuming a constant N:C ratio of 144 for the range of nitrate concentrations typically found in the Mediterranean Sea (e.g., Siokou-Frangou et al., 2010).

$$rfr_{LoF} = \frac{6.9 * PO_3 + 6}{144}$$; Eq. 3

With these variable ratio the molar composition of the OM changes depending on the chemical composition of the environment (i.e, the phosphate concentration) as shown in Fig. 3 below. With low phosphate concentration in the water the produced OM has higher-than-Redfield N:P molar ratio (up to a maximum ~ 24) while with high phosphate concentration the $N:P_{OM}$ can go below Redfield. Of course, this has an implication also on the determination of the limiting nutrient, as for each PO_3 concentration in the water the threshold for nitrate or phosphate limitation changes.

Figure 3. Dependence of the N:P_{OM} with the waters' PO3 concentration following Eq. 3

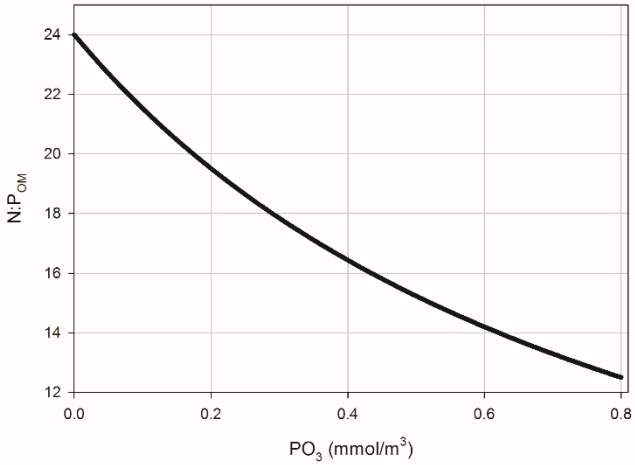

The simple implementation shown in Eq. 3 allows, thus, to consider the known flexibility phytoplankton shows for different chemical conditions regarding nutrients. The changes shown in Fig. 3 could come from intra-specific flexibility of the phytoplankton cells or from changes in the community composition as a response to variable nutrients conditions.

We perform two twin-simulations covering the period 2000 – 2007 (only data from 2001 onwards were considered). The first one assumes the Redfield ratio in the nutrients' assimilation rate (RfR simulation) while the second uses the LoF relationship shown in Eq. 3 (LoF simulation). All other conditions (initial values, boundaries, external forcings, etc..) are exactly the same in the two simulations.

3 Results

3.1 Surface chemical conditions

We can now look at how the use of a fixed or variable N:P ratio in phytoplankton uptake affects the surface chemical conditions in the basin. Figure 4 shows the mean climatological surface concentrations of the two major nutrients in the water, nitrate and phosphate. If we start looking at the nitrate concentrations (Fig. 4A and 4B), it is clear that in the LoF run, mean surface values are much lower than in the RfR (0.56 mmol/m^3 vs 1.13 mmol/m^3). Regarding spatial distributions, for the RfR a north-south gradient is quite evident with not very large differences between western and eastern basin (maximum mean surface concentrations of ~2 mmol/m^3 being found in both regions). On the opposite, in the LoF run surface nitrate is more scarce in the eastern basin (maximum concentration ~ 0.5 mmol/m^3) than in the western one (maximum ~ 1.8 mmol/m^3) while still a certain north-south gradient is present. Both, spatial distribution and absolute values are much more similar to reported values in the LoF run than in the RfR run (see section 3.3 below).

Figure 4. Mean climatological surface (10m) nutrients concentrations in water (mmol/m3). Upper row, nitrate. Middle row, phosphate. Lower row, N:P molar ratio. Left column RfR simulation. Right column, LoF simulation.

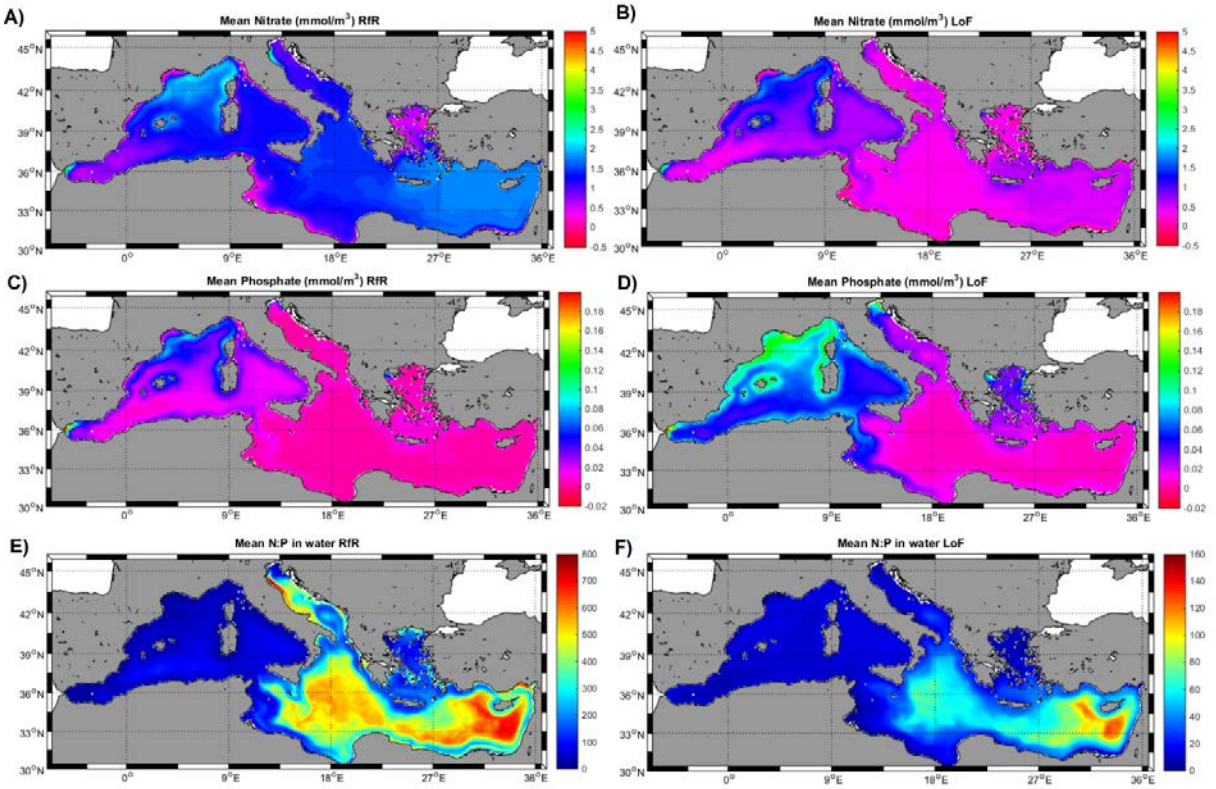

For phosphate the situation is quite the opposite (Fig. 4C and 4D) as mean concentration is higher in LoF (~ 0.036 mmol/m^3) than in the RfR run (~0.014 mmol/m^3). A similar north-west to south-east gradient could be seen in both distribution maps with some large differences in marginal basins such as the Adriatic, the Aegean and the Gulf of Gabes region where phosphate is quite higher in the LoF run (Fig. 4D).

As a consequence of the patterns described above, the N:P ratios in the water for each simulation are quite different. Mean $N:P_{water}$ is ~ 250 for the RfR run and ~ 30 for the

LoF. In both cases, though, a gradient towards the south-east is quite evident (see Fig. 4E and 4F) with the N:P_{water} reaching very large values in the easternmost region of the basin. As commented before, the mean values of the ratio and its spatial distribution agrees better with previous reports for the LoF run than for the RfR (see section 3.3) as in this later case a combination of very high nitrate in the water with very low phosphate makes this ratio to reach unrealistically high values (see Fig. 4E).

The side by side comparison of N:P_{water} in both model runs (Fig. 5) shows clearly that LoF simulates a lower value than RfR in the entire Mediterranean (map in Fig. 5) but with a clear longitudinal gradient (lower panel Fig. 5), being the difference much larger in the eastern part of the basin.

Figure 5. Upper panel, N:P in water anomalies (LoF – RfR runs). Lower panel, longitudinal means of the N:P in water anomalies.

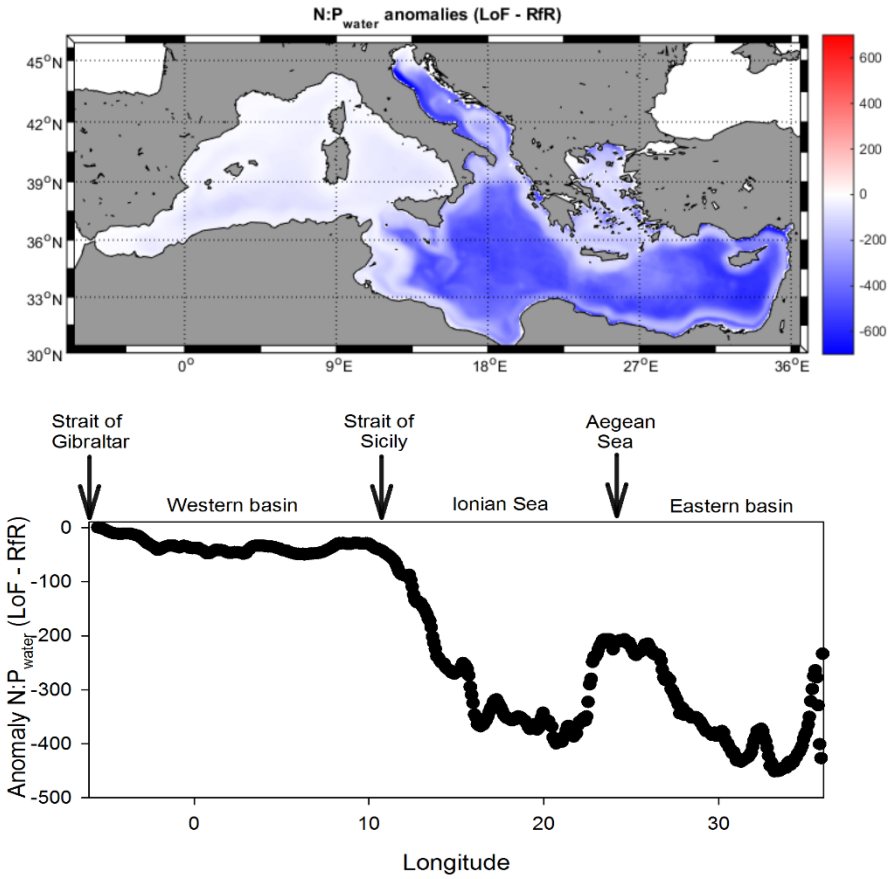

We can have a look at how the N:P ratio in the organic matter is distributed in the LoF (remember that for RfR this is fixed to 16). The mean map of N:P_{OM} is shown in Fig. 6A where a north-west to south-east ratio is clearly seen as also shown in the longitudinal mean in Fig. 6B. Mean value of this ratio for the entire basin is ~22.4, i.e. higher than Redfield.

Figure 6. A) Mean climatological molar N:P ratio in organic matter (OM) for the LoF simulation (for the RfR it is set to 16). B) longitudinal mean of the N:P mean ratio shown in the map.

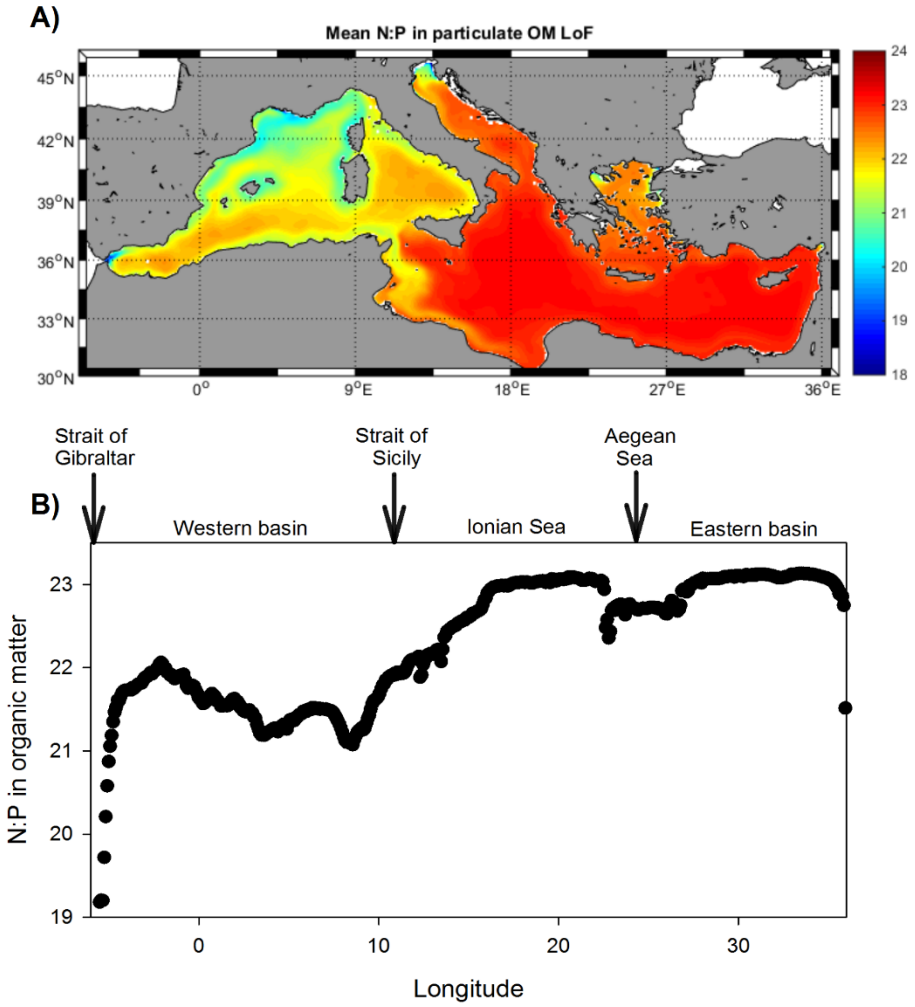

The correlation between the $N:P_{water}$ (i.e., the map in Fig. 4F) and the $N:P_{OM}$ (i.e., the map in Fig. 6A) for the LoF run is shown in Fig. 7. A positive relationship is evident, with higher $N:P_{OM}$ happening in regions with high $N:P_{water}$. This relationship is an obvious consequence of the LoF implementation as shown by Eq. 3.

There is, however, a deviation of this general pattern happening at $N:P_{water}$ ~16 (i.e., the Redfield ratio) where a small cloud of points showing the opposite trend are located (red dots in the intermediate plot in Fig. 7). The location of these data is shown in the small map of the figure (red areas) corresponding to highly productive regions where new nutrients inputs typically happen; by the entrance of Atlantic waters through the Strait of Gibraltar or by the intense vertical mixing caused by the mesoscale activity and by the winter deep convection in the NW Mediterranean. In both regions, waters with a much lower N:P signature (~16 for the Atlantic and ~17 for the Gulf of Lion region) are supplied to the euphotic layer which seems to have a large effect on the N:P of the organic matter produced as result.

Figure 7. Scatter plot of N:P in OM versus N:P in water for the LoF run. The map in the inlet shows the region from where the red dots come from.

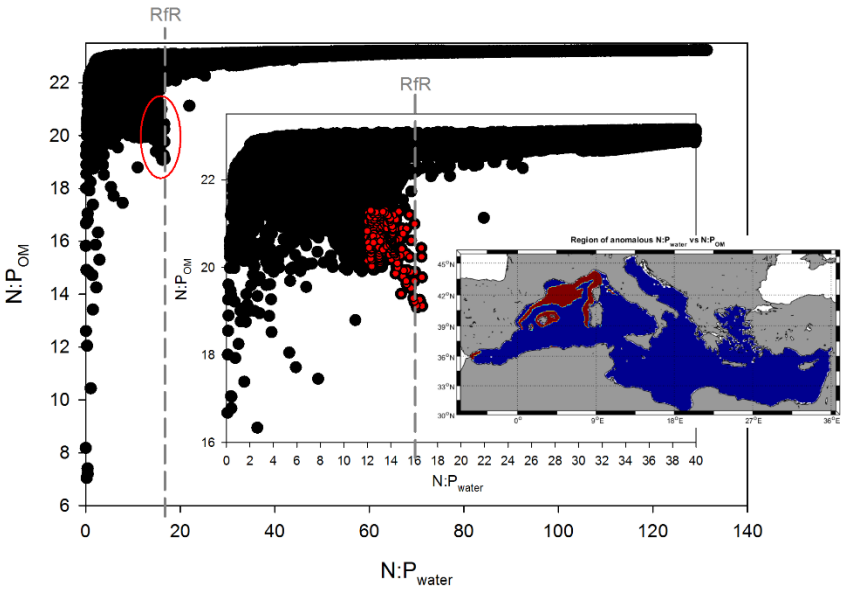

3.2 Vertical patterns

From previous modelling works (e.g., Macias et al., 2014a) it has become clear that the vertical distribution of biogeochemical variables is an important factor for the ecological status of the pelagic ecosystem in the Mediterranean Sea, especially during the stratification period when extreme oligotrophic conditions are stablished in the uppermost layers.

Thus, it is relevant to test if the inclusion of the variable N:P ratio in phytoplankton uptake has any effect on the vertical distribution of biogeochemical variables. For doing this we have extracted the vertical profiles from the two model runs in the two open-water regions detailed in Macias et al. (2014a), one in the western basin and another in the eastern basin. Climatological vertical profiles of the different variables are then computed and plotted in Figs. 8 and 9.

Starting with the western basin (Fig. 8), the effects on nutrients' vertical distributions of the variable N:P ratio is quite significant. For nitrate, surface values are largely reduced in the LoF (Fig. 8B) with larger intermediate values (~120m) increasing, thus, the vertical gradient. For phosphate, surface values increase during winter and spring and deeper values (~100 – 150 m) increase during the whole year (Fig. 8D). As a result, the $N:P_{water}$ ratio decreases largely in the LoF run (Fig. 8F) with the strong limitation by phosphate only happening during the central months of the summer in the uppermost layers of the water column (<50m).

Figure 8. Vertical climatological distributions of biogeochemical variables at the open-sea western area for the RfR run (left column) and for the LoF run (right column).

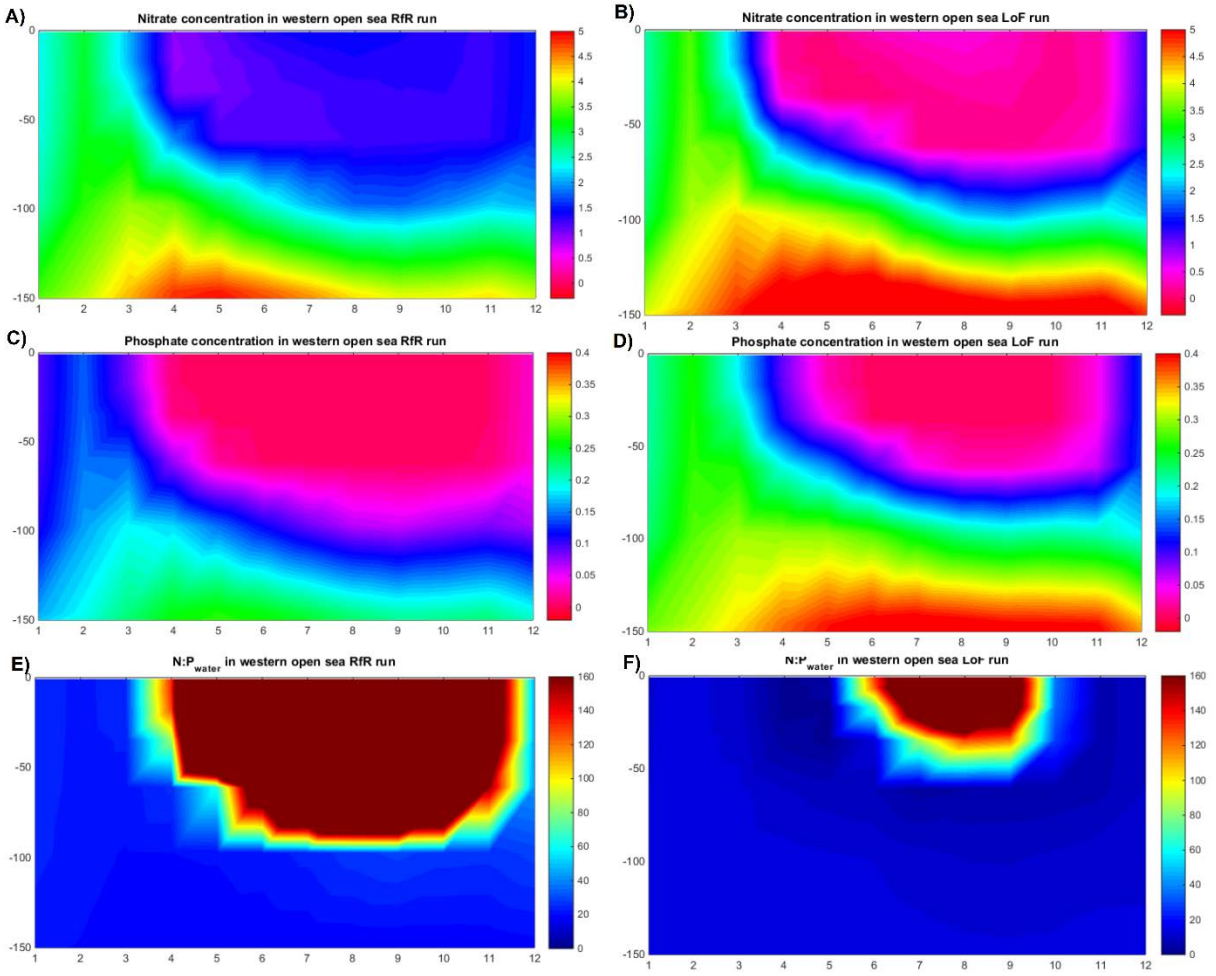

For the eastern Mediterranean (Fig. 9), the effect of LoF in the nitrate concentration is quite large (Fig. 9A and 9B). While in the RfR upper-water (up to ~100m) nitrate levels are quite high (~1.5 mmol/m^3) and seems to come from a surface source during winter (see Fig. 9A), for the LoF surface levels are greatly reduced (to an average of ~ 0.5 mmol/m^3) and the spatio-temporal pattern seems to be more linked with a deep source of fertilization during winter months. Phosphate concentration in surface waters is not much changed up to ~120m although at deeper levels LoF simulates higher average values (Figs. 9C and 9D). $N:P_{water}$ ratio is always extremely high in the RfR simulation (Fig. 9E) while it presents a clear seasonality in the LoF run (Fig. 9F) with maximum values during the stratification season in surface (<75m) waters.

Figure 9. Vertical climatological distributions of biogeochemical variables at the open-sea eastern area for the RfR run (left column) and for the LoF run (right column).

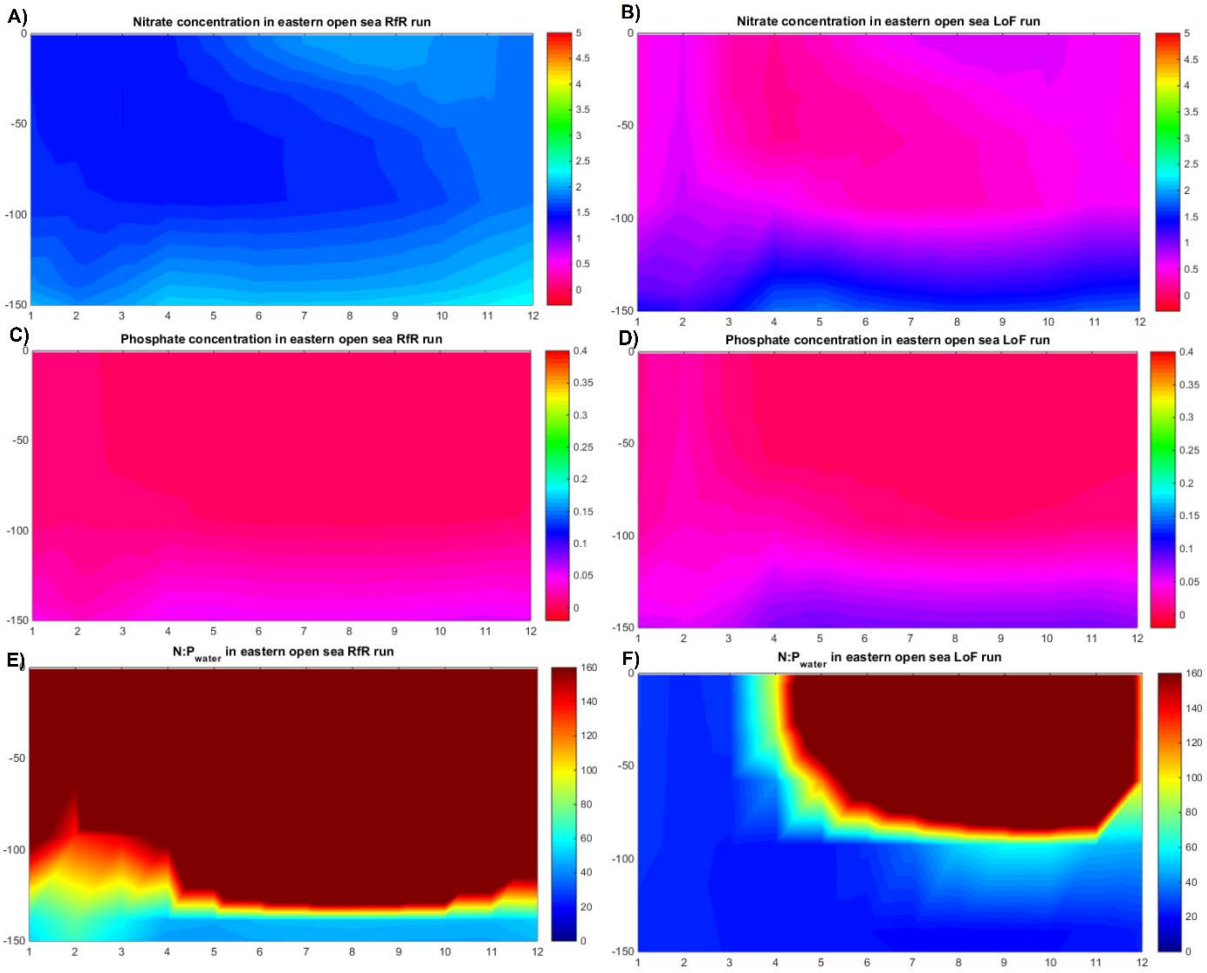

3.3 Model validation

In this section model results will be compared with available data on nutrients distribution in the Mediterranean Sea. Both, horizontal patterns, seasonal cycles and different depth horizons will be analysed.

We will start with the general comparison of mean nutrients values in the two analysed 'boxes' (NW Med & Eastern Med) for the two model runs with the results by Powley et al. (2017). From the numbers in Table 1, it could be seen that in general both RfR and LoF provides mean values that are within the range of reported values (bracketed figures in table 1). However, it is quite clear that surface values of nitrate in the RfR are substantially larger than in the LoF, especially for the Eastern Mediterranean. Such values are still within the range of observations provided by Powley et al. (2017) but they are almost three times larger than the 'stable' value found in their modelling exercise.

Phosphate values in both model runs are in general comparable to values reported elsewhere, including observational data and model simulations.

Table 1. Comparison of mean integrated values of nitrate and phosphate in different 'boxes' and water depth horizons as defined in Powley et al., 2017.

Sub-basin	Depth	**NO_3** RfR LoF (*min – max*) Powley et al (2017)	**PO_4** RfR LoF (*min – max*) Powley et al (2017)
WM	**SW** (surface)	1.74 1.3 (*0 – 7.3*) 0.8	0.045 0.11 (*0 – 0.35*) 0.05
	IW (interm)	6.4 7.2 (*1.4 – 9.9*) 6.6	0.36 0.47 (*0.04 – 0.47*) 0.26
	DW (deep)	8.0 8.3 (*1.6 – 9.5*) 7.7	0.44 0.48 (*0.14 – 0.48*) 0.37
EM	**SW** (surface)	1.85 0.8 (*0.01 – 3*) 0.6	0.018 0.007 (*0 – 0.1*) 0.02
	IW (interm)	3.76 3.9 (*0.5 – 6*) 2.6	0.14 0.16 (*0.03 – 0.2*) 0.102
	DW (deep)	4.65 4.7 (*3 – 6*) 4.8	0.16 0.17 (*0.13 – 0.23*) 0.17

It is a challenge to obtain meaningful, comprehensive distribution maps of nutrients in the Mediterranean Sea due to the scarcity of observational data. However, we will use here the data contained in the World Ocean Atlas (WOA13) for a spatially-explicit comparison with both model runs (Fig. 10).

Figure 10. Horizontal comparison of surface nitrate in the WOA13 and in the two model runs. A) Mean climatological surface nitrate concentration in WOA13. B) Mean climatological surface nitrate anomaly (RfR – WOA13). C) Mean climatological surface nitrate anomaly (LoF – WOA13). C) Longitudinal mean surface nitrate concentration in the WOA13 and in the two model runs.

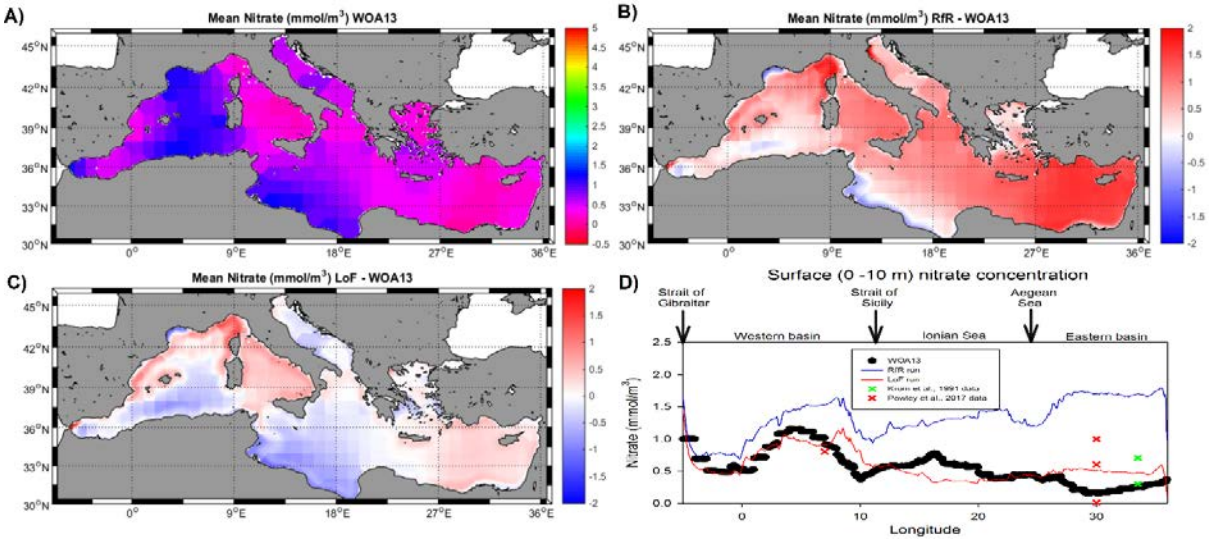

The mean surface nitrate concentration from WOA13 (Fig. 10A) does resemble the pattern shown in Fig. 4 from the two model runs with a general west to east gradient and localized maximum in the NW region. The RfR mean surface values (Fig. 4A) are generally larger than those in WOA13 as confirmed by the anomalies map in Fig. 10B (mean anomaly RfR – WOA13 ~ 0.78 mmol N/m^3) and by the longitudinal means shown in Fig. 10D. Indeed, the RfR surface nitrate tends to increase within the Eastern basin, a pattern not expected and not reported elsewhere. Also, RfR values (blue line in Fig. 10D) are outside reported values in other experimental works (coloured crosses in Fig. 10D). The comparison between WOA13 and LoF simulation is much better (Fig. 10C) with a mean anomaly of just -0.004 mmolN/m^3. Also the longitudinal distribution of surface nitrate for the LoF (red line in Fig. 10D) is much closer to the WOA13 data (black circles in Fig. 10D) and within the limits of the other observational data (coloured crosses in Fig. 10D).

Figure 11. Horizontal comparison of surface phosphate in the WOA13 and in the two model runs. A) Mean climatological surface phosphate concentration in WOA13. B) Mean climatological surface phosphate anomaly (RfR – WOA13). C) Mean climatological surface phosphate anomaly (LoF – WOA13). C) Longitudinal mean surface phosphate concentration in the WOA13 and in the two model runs.

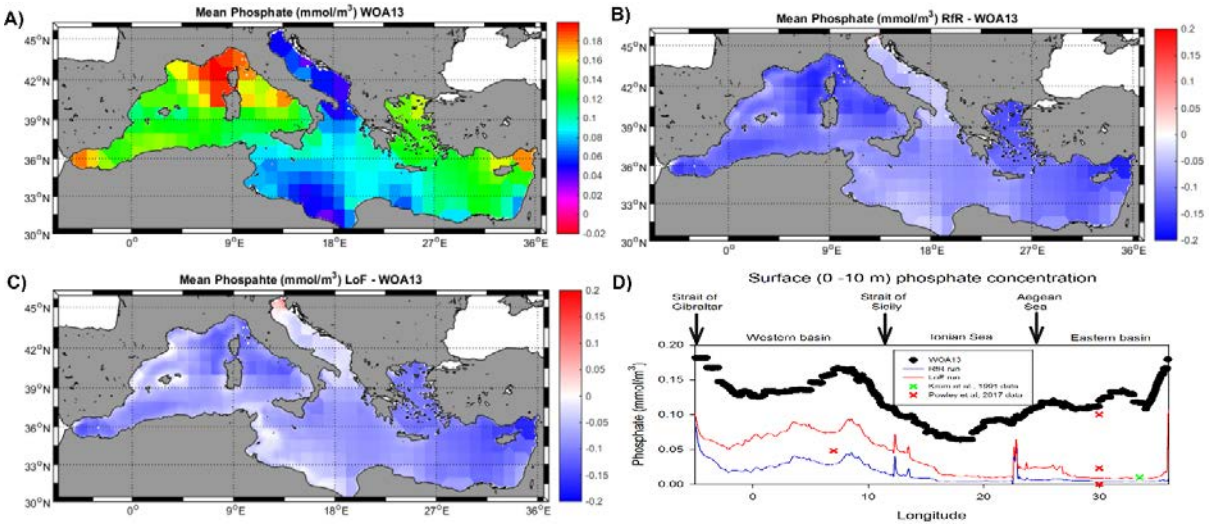

Surface phosphate concentration values from WOA13 (Fig. 11A) are larger than those obtained from the two model runs (Fig. 4C and 4D). This is corroborated by the anomaly maps shown in fig. 11B and 11C with mean anomalies of -0.09 mmol P/m^3 for RfR and of -0.075 mmol P/m^3 for LoF. The same type of anomalies could be observed in the longitudinal means shown in Fig. 11D, where WOA13 values (black circles) are always larger than model simulations (coloured lines). However, WOA13 phosphate values are also outside the range of observed values from other works (coloured crosses in Fig. 11D) and, indeed, if the N:P_{water} ratio is computed from the WOA13 surface values a mean value of 5.98 is obtained for the whole Mediterranean. This value of the N:P_{water} ratio is much lower than the general oceanic RfR and very small compared with typical values for the Mediterranean (e.g., Krom et al., 1991; Marty et al., 2002; Tanaka et al., 2010; Powley et al., 2017). All these facts made the surface phosphate values contained in the WOA13 database to be considered with caution in the comparison with model data.

Figure 12. Climatological vertical profiles of A) Nitrates, B) Phosphate and C) N:P_{water} for the different model runs (RfR, blue lines & LoF, red lines) and diverse databases (WOA, black symbols; Krom et al., 1991; green symbols; Powley et al., 2017, red symbols) in the two analyzed regions of the Mediterranean (NW & Eastern).

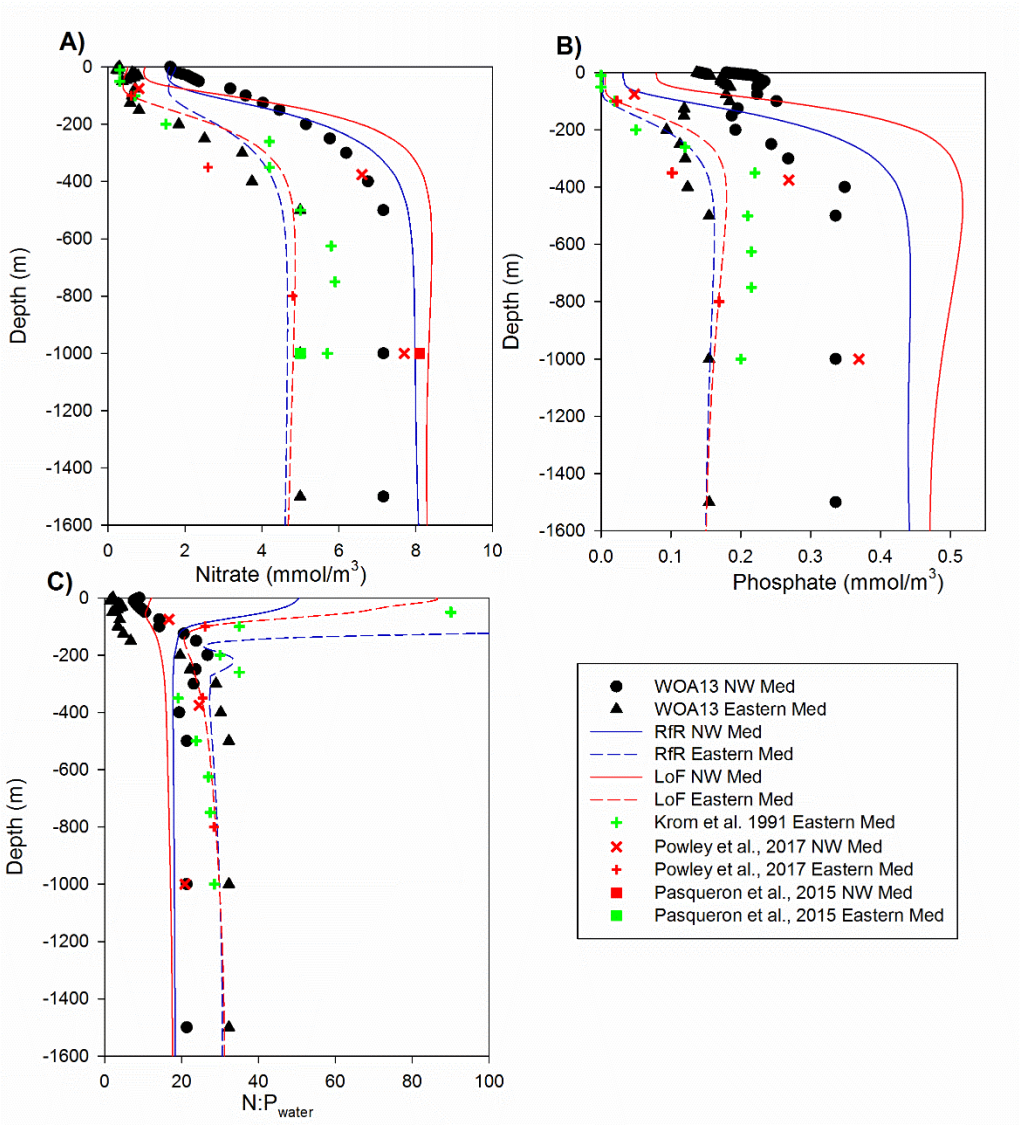

Vertical climatological profiles of the two nutrients are shown in Fig. 12. If we start with the deepest part of the basin, a west to east gradient could be clearly seen in both nitrate and phosphate, all data and model runs show higher nutrients concentrations in the west than in the east. The agreement between model simulations and data is high for both RfR and LoF although in the west model figures for phosphate are slightly larger than observations (~+0.1 mmol P/m^3). The deep concentration is quite invariable up to a depth of ~500m in both model and data and for the two studied regions. From that point to the surface nutrients concentrations sharply decrease to a surface minimum. At surface the same west-east gradient is observed, with larger values in the NW Med and lower in the East. For nitrate it is evident that the LoF surface values are closer to observations than those of the RfR run (Fig. 12A) especially for the Eastern Mediterranean. The comparison with surface values for phosphate is more tricky (Fig. 12B) because of the already mentioned possible overestimation of the WOA13 values. However, both model runs show surface values within the range of observations for both regions.

If we now look at the N:Pwater ratio (Fig. 12C), both model runs show very similar values in the deep part of the basin, being at ~18 in the NW Med and ~ 29 in the Eastern Med, in line with databases and previous observations. These values are quite constant up to a depth of ~ 300m in the Eastern Med and ~ 200m in the NW Med (Fig. 12C) where significant differences between the two model runs start to appear. For the RfR in

the NW Med (continuous blue line in Fig. 12C) the $N:P_{water}$ at surface increases from 18 to ~50 while for the LoF run (continuous red line in Fig. 12C) the ratio value slightly decrease to ~12. Available data (with the cautious remark given to WOA13) seems to indicate the value of the LoF as the most likely one. For the Eastern Med both model simulations (discontinuous lines in Fig. 12C) increase up to ~80 in LoF and over 200 in RfR. Again, model-data comparison seem to be better when the LoF results are considered.

The basic same conclusion could be drawn from the comparison of climatological surface (0-30m) and deep (900-1100m) nitrate values at the two studied sites shown in Fig. 13. Deep values (Fig. 13B) are fairly well represented in both model runs and for the two sites, at ~ 4.9 mmol N/m^3 in the Eastern Med and at ~ 8 mmol N/m^3 in the NW Med. Surface values show, again, that RfR values are too high in both places, especially in the Eastern Med and during the stratification period. On the contrary, LoF nitrate concentrations closely follow the seasonal cycle in both areas with minimum deviation with respect historical values.

Figure 13. Climatological nitrate values in surface (0-30 m) and deep (900 -1100 m) layers of the NW and Eastern Mediterranean Sea from both model runs (coloured lines) and from the historical data reported in Fommervault et al. (2018).

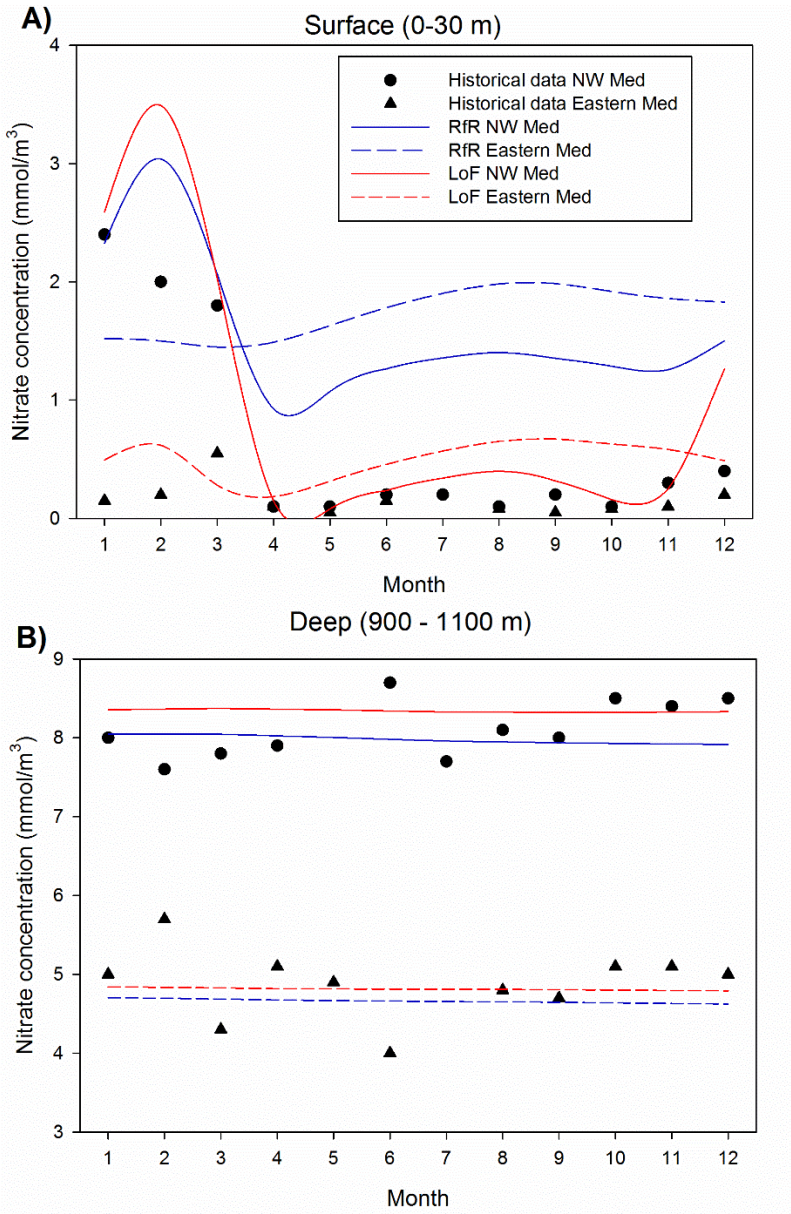
A)
Surface (0-30 m)
Historical data NW Med
Historical data Eastern Med
RfR NW Med
RfR Eastern Med
LoF NW Med
LoF Eastern Med
Nitrate concentration (mmol/m3)
Month
B)
Deep (900 - 1100 m)
Nitrate concentration (mmol/m3)
Month

4 Discussion

4.1 Effects on dissolved nutrients concentrations

As shown in the extensive results exposition above, the main effect of using a variable $N:P_{OM}$ ratio with respect to the more classical, fixed RfR value in the Mediterranean Sea is to reduce the levels of free nitrogen in the surface waters and slightly increase the surface phosphate concentrations. The comparison with available data done in the previous section (section 3.3) indicates that the surface nitrate levels in the RfR simulations are far too high, especially on the Eastern Med as typically reported values there range between 0.3 – 0.7 mmol /m^3 (e.g., Krom et al., 1991; Powley et al., 2017) while RfR simulated values are ~1.8 mmol/m^3. Indeed, Pasqueron de Fommervault et al. (2015) shows from historical nitrate measurements covering the period 1961 – 2010 that surface values in the Levantine basin never arrives over 0.5 mmol N/m^3, so RfR values for this region are clearly overestimated.

The longitudinal comparisons between observed and simulated nutrients values done in panel C of Figs. 10 & 11 confirm that the RfR surface nitrate is too large while in the LoF run simulated concentrations are within the observational range for the entire basin. The effects on phosphate are much smaller and, in both cases (RfR and LoF), simulated surface concentrations remain within reported values.

The reduction in free-nitrate in water when a variable internal N:P ratio is adopted in the model agrees with the results Fransner et al. (2018) obtained for the Gulf of Bothnia. In their 'FIX' simulation (corresponding to our RfR) the consumption of dissolved inorganic nitrogen was not high enough to bring simulated values close to observations (see their Fig. 5 and also Edman and Anderson, 2014) while when a variable ratio was introduced to the model, free nitrogen levels decreased. They also found out that in the variable internal ratio run, the amount of free phosphate in the surface waters increased with respect to the fixed ratio, in agreement with our own results.

Simulated deep water values are not very much affected by the selected approach in the internal nutrient ratios (see Figs. 12 & 13) and correspond to the reported values elsewhere. Both deep nitrate and phosphate concentrations are approximately twice in the western basin (nitrate ~ 8.0; phosphate ~ 0.4) than in the eastern (nitrate ~ 4.4; phosphate ~ 0.16) Mediterranean as previously reported (Moutin & Raimbault, 2002; Pujo-Pay et al., 2011).

$N:P_{water}$ is lower in the NW Med in both simulations at a value ~ 18 (Bethoux et al., 1992; Marty et al., 2002; Pujo-Pay et al., 2010) while $N:P_{water}$ is larger in the eastern region with a value ~ 30 in both simulations (Krom et al., 1991; Kress & Herut, 2001; Pujo-Pay et al., 2010). What does change from RfR to LoF is the slope of the nitracline, much sharper in the later simulation due to the decrease in surface values (see Fig. 12A).

4.2 Effects on organic matter composition

Fig. 6 shows clearly how the $N:P_{OM}$ ratio increases from west to east following the phosphate gradient (inversely). This increase of the ratio with decreasing phosphate levels is a direct consequence of the implementation of the LoF approach (Eq. 3) and agrees with the reported fact that phytoplankton can be economical with their phosphorous requirements when supply is limited (e.g., DeVries & Deutsch, 2014). It also agrees with the findings of Tanaka et al. (2011) and Krom et al. (2014) based on field data measurements and with the theoretical map shown by G-M15 (their figure 2, lower panel).

Our maximum values of $N:P_{OM}$ are ~24, much lower than those obtained by Fransner et al. (2018) for the northern Baltic Sea. However, we have to stress here that our LoF implementation (Eq. 3) only allows $N:P_{OM}$ to reach a maximum of 24 (corresponding to 0 phosphate concentration, see Fig. 3) and also that Fransner et al. (2018) maximum ratio could be overestimating the real value as they do recognize themselves (max observed values in the Gulf of Bothnia ~ 21, Pertola et al., 2002).

The largest differences in the $N:P_{water}$ between both runs (Fig. 5) are simulated in the region where $N:P_{OM}$ is larger in the LoF run (Fig. 6) with a clear significant correlation between both variables (Fig. 7). Again, this pattern indicate that the highest impact of the LoF approach on dissolved nutrients happens in phosphate depleted regions due to the added plasticity in the internal cell dynamics that this formulation allows. This agrees with the proposed hypothesis that under phosphorous limitation a core biogeochemistry with high N:P ratios is more advantageous for the cells (Loladze & Elser, 2011).

4.3 Concluding remarks

The relatively simple modification to a low-complexity biogeochemical model allows to account for the internal planktonic plasticity in nutrients dynamics that is typically only considered by highly complex, multi-compartment models (*e.g.,* Vichi et al., 2007). Our simpler approach is much more cost-effective in terms of computational running time (the LoF modification does not add any computing time) and it seems to be appropriate for the description of the Mediterranean Sea chemical environment (with respect to dissolved nutrients).

Getting an adequate description of the amount of free inorganic nutrients in marine waters from model simulations is a requisite, for example, to use eutrophication indexes that incorporate such variable (e.g., Stips et al., 2016). The inclusion of the LoF in MedERGOM is shown to make model predictions of surface inorganic nutrients in water closer to observed values constitutes, thus, a beneficial modification when planning to use this model to assess ecosystem status in the basin (Cardoso et al., 2010).

References

Ayata, S.D., Levy, M., Aumont, O., Resplandy, L., Tagliabue, A., Sciandra, A., Bernard, O., 2014. Phytoplankton plasticity drives large variability in carbon fixation efficiency. Geophysical Research Letters, 41: 8994–9000.

Baretta, J.W., Ebenhoh, W., Ruardij, P., 1995. The European regional seas ecosystem model, a complex marine ecosystem model. Netherlands Journal of Sea Research, 33: 233–246.

Bauer, J.E., Cai, W.J., Raymond, P.A., Bianchi, T.S., Hopkinson, C.S., Regnier, P.A.G., 2013. The changing carbon cycle of the coastal ocean. Nature, 504((7478)): 61-70.

Béthoux, J.P., Morin, P., Madec, C., Gentili, B., 1992. Phosphorus and nitrogen behaviour in the Mediterranean Sea. Deep-Sea Research. Part A Oceanogr. Res. Papers, 39(9): 1641–1654.

Béthoux, J.P., Morin, P., Chaumery, C., Connan, O., Gentili, B., Ruiz-Pino, D., 1998. Nutrients in the Mediterranean Sea, mass balance and statistical analysis of concentrations with respect to environmental change. Marine Chemistry, 63: 155-169.

Béthoux, J.P., Morin, P., Ruiz-Pino, D.P., 2002. Temporal trends in nutrient ratios: chemical evidence of Mediterranean ecosystem changes driven by human activity. Deep-Sea Research II, 49: 2007-2016.

Blackford, J.C., Allen, J.I., Gilbert, F.J., 2004. Ecosystem dynamics at six contrasting sites: A generic modelling study. Journal of Marine Systems, 52(1-4): 191–215.

Bruggeman, J., Bolding, K., 2014. A general framework for aquatic biogeochemical models. Environ. Modell. Software, 61: 249-265.

Burchard, H., Bolding, K., 2002. GETM, a general estuarine transport model, European Commission, Ispra, Italy.

Cardoso, A.C., and others., 2010. Scientific support to the European Commission on the Marine Strategy Framework Directive. Management Group Report, European Commission, Luxemburg.

DeVries, T., Deutsch, C., 2014. Large-scale variations in the stoichiometry of marine organic matter respiration. Nature Geoscience, 7: 890-894.

Elser, J.J., Fagan, W.F., Denno, R.F., Dobberfuhl, D.R., Folarin, A., Huberty, A., Interlandi, S., Kilham, S.S., McCauley, E., Schulz, K.L., Siemann, E.H. and Sterner, R.W., 2000. Nutritional constraints in terrestrial and freshwater food webs. Nature, 408: 578.

Falkowski, F.G., 2000. Rationalizing elemental ratios in unicellular algae. J. Phycol., 36: 3-6.

Flynn, K.J., 2010. Ecological modelling in a sea of variable stoichiometry: Dysfunctionality and the legacy of Redfield and Monod. Prog. Oceanog., 84(1-2): 54-65.

Fransner, F., Gustafsson, E., Tedesco, L., Vichi, M., Hordoir, R., Roquet, F., Spilling, K., Kuxnetsov, I., Eilola, K., Morth, C.M., Humborg, C., Nycander, J., 2018. Non-Redfieldian Dynamics Explain Seasonal pCO2 Drawdown in the Gulf of Bothnia. Journal of Geophysical Research, 123.

Galbraith, E.D., Martiny, A.C., 2015. A simple nutrient-dependence mechanism for predicting the stoichiometry of marine ecosystems. Proc. Natl. Acad. Sci. USA, 112(27): 8199-8204.

Geider, R.J., La Roche, J., 2002. Redfield revisited: variability of C:N:P in marine microalgae and its biochemical basis. Eur. J. Phycol., 37: 1-17.

Gruber, N., Sarmiento, J.L., 1997. Global patterns of marine nitrogen fixation and denitrification. Global Biochemical Cycles, 11: 235–266.

Karpinets, T., Greenwood, D., Sams, C., Ammons, J., 2006. RNA:protein ratio of the unicellular organism as a characteristic of phosphorous and nitrogen stoichiometry and of the cellular requirement of ribosomes for protein synthesis. BMC Biol., 4: 30.

Klausmeier, C.A., Litchman, E., Daufresne, T. and Levin, S.A., 2004. Optimal nitrogen-to-phosphorus stoichiometry of phytoplankton. Nature, 429: 171.

Kress, N., Herut, B., 2001. Spatial and seasonal evolution of dissolved oxygen and nutrients in the southern Levantine Basin (eastern Mediterranean Sea): Chemical characterization of the water masses and inferences on the N:P ratios. Deep-Sea Research I, 48(11): 2347–2372.

Krom, M.D., Kress, N., Brenner, S., 1991. Phosphorous limitation of primary productivity in the eastern Mediterranean Sea. Limnol. Oceanogr., 36(3): 424-432.

Krom, M.D., Herut, B., Mantoura, R.F.C., 2004. Nutrient budget for the Eastern Mediterranean: implications for P limitation. Limnol. Oceanogr., 49: 1582-1592.

Krom, M.D., Emeis, K.C., Van Cappellen, P., 2010. Why is the Eastern Mediterranean phosphorus limited? Progress in Oceanography, 85: 236-244.

Krom, M.D., Kress, N., Berman-Frank, I., Rahav, E., 2014. Past, present and future patterns in the nutrient chemistry of the eastern Mediterranean. In: S.G.a.Z. Dubinsky (Editor), The Mediterranean Sea. Its History and Present Challenges. Springer, Dordrecht, Netherlands.

Loladze, I., Elser, J.J., 2011. The origins of the Redfield nitrogen-to-phosphorus ratio are in a homoeostatic protein-to-rRNA ratio. Ecology Letters, 14: 244-250.

Ludwig, W., Dumont, E., Meybeck, M., Heussner, S., 2009. River discharges or water and nutrients to the Mediterranean and Black Sea: Major drivers for ecosystem changes during past and future decades? Prog. Oceanog., 80: 199-217.

Macías, D., García-Gorríz, E., Stips, A., 2013. Understanding the Causes of Recent Warming of Mediterranean Waters. How Much Could Be Attributed to Climate Change? Plos One, 8(11): e81591.

Macías, D., García-Gorríz, E., Piroddi, C., Stips, A., 2014. Biogeochemical control of marine productivity in the Mediterranean Sea during the last 50 years. Global Biochemical Cycles, 28: 897-907.

Macías, D., Stips, A., Garcia-Gorriz, E., 2014. The relevance of deep chlorophyll maximum in the open Mediterranean Sea evaluated through 3D hydrodynamic-biogeochemical coupled simulations. Ecol. Model., 281: 26-37.

Macías, D., García-Gorríz, E., Stips, A., 2017. Major fertilization sources and mechanisms for Mediterranean Sea coastal ecosystems. Limnol. Oceanogr., In press.

Marty, J.C., Chiaverini, J., Pizay, M.D., Avril, B., 2002. Seasonal and interannual dynamics of nutrients and phytoplankton pigments in the western Mediterranean Sea at the DYFAMED time-series station (1991–1999). Deep-Sea Research II, 49(11): 1965–1985.

Moutin, T., Raimbault, P., 2002. Primary production, carbon export and nutrients availability in western and eastern Mediterranean Sea in early summer 1996 (MINOS cruise). Journal of Marine Systems, 33: 273–288.

Neumann, T., 2000. Towards a 3d-ecosystem model of the Baltic Sea. Journal of Marine Systems, 25: 405-419.

Pantoja, S., Repeta, D.J., Sachs, J.P., Sigman, D.M., 2002. Stable isotope constraints on the nitrogen cycle of the Mediterranean water column. Deep-Sea Research I, 49: 127-142.

Pasqueron de Fommervault, O., D'Ortenzio, F., Mangin, A., Serra, R., Migon, C., Claustre, H., Lavigne, H., Ribera d'Alcala, M., Prieur, L., Taillandier, V., Schmechtig, C., Poteau, A.,

Leymarie, E., Dufor, A., Besson, F., Obolensky, G., 2015. Seasonal variability of nutrient concentrations in the Mediterranean Sea: Contribution of Bio-Argo floats. Journal of Geophysical Research Oceans, 120: 8528-8550.

Pertola, S., Koski, M., Viitasalo, M., 2002. Stoichiometry of mesozooplankton in N- and P-limited areas of the Baltic Sea. Marine Biology, 140: 425–434.

Powley, H.R., Krom, M.D., Van Cappellen, P., 2017. Understanding the unique biogeochemistry of the Mediterranean Sea: Insights from a coupled phosphorus and nitrogen model. Global Biochemical Cycles, 31: 1010-1031.

Pujo-Pay, M., Conan, P., Oriol, L., Cornet-Barthaux, V., Falco, C., Ghiglione, J.F., Goyet, C., Moutin, T., Prieur, L., 2011. Integrated survey of elemental stoichiometry (C, N, P) from the western to eastern Mediterranean Sea. Biogeosciences, 8(4): 883–899.

Redfield, A.C., 1934. On the proportions of organic derivations in sea water and their relation to the composition of plankton. In: R.J. Daniel (Editor), James Johnstone Memorial Volume. University Press of Liverpool, pp. 177-192.

Ribera d'Alcalá, M., Civitarese, G., Conversano, F., Lavezza, R., 2003. Nutrient fluxes and ratios hint at overlooked processes in the Mediterranean sea. J. Geophys. Res., 108: 8106.

Richon, C., Dutay, J.C., Dulac, F., Wang, R., Balkanski, Y., Nabat, P., Aumont, O., Desboeufs, K., Laurent, B., Guieu, C., Raimbault, P., Beuvier, J., 2018. Modeling the impacts of atmospheric deposition of nitrogen and desert dust-derived phosphorus on nutrients and biological budgets of the Mediterranean Sea. Prog. Oceanog.

Sarmiento, J.L., Herbert, T., Toggweiler, J.R., 1988. Mediterranean nutrient balance and episodes of anoxia. Global Biochemical Cycles, 2: 427–444.

Siokou-Frangou, I., Christaki, U., Mazzocchi, M.G., Montresor, M., Ribera d'Alcalá, M., Vaqué, D., Zingone, A., 2010. Plankton in the open Mediterranean Sea: a review Biogeosciences, 7: 1543-1586.

Sterner, R.W., Elser, J.J., 2002. Ecological Stoichiometry: The Biology of Elements From Molecules to the Biosphere. Princeton University Press, Princeton.

Stips, A., Bolding, K. ,Pohlman, T., Burchard, H., 2004. Simulating the temporal and spatial dynamics of the North Sea using the new model GETM (general estuarine transport model). Ocean Dynamics, 54: 266-283.

Stips, A., Dowell, M., Somma, F., Coughla, C., Piroddi, C., Bouraoui, F., Macias, D., Garcia-Gorriz, E., Cardoso, A.C., Bidoglio, G., 2015. Towards an integrated water modelling toolbox, European Commission, Luxemburg.

Stips, A., Macias, D., Garcia-Gorriz, E., Miladinova, S., 2016. Alternative assessments of large scale Eutrophication using ecosystem simulations: hind-casting and scenario modelling, European Commission, Luxemburg.

Tagliabue, A., Arrigo, K.R., 2005. Iron in the Ross Sea: 1. Impact on CO2 fluxes via variation in phytoplankton functional group and non-Redfield stoichiometry. J. Geophys. Res., 110: C03009.

Tanaka, T., Thingstad, T.F., Christaki, U., Colombet, J., Cornet-Barthaux, V., Courties, C., Grattepanche, J.-D., Lagaria, A., Nedoma, J., Oriol, L., Psarra, S., Pujo-Pay, M., Van Wambeke, F., 2011. Lack of P-limitation of phytoplankton and heterotrophic prokaryotes in surface waters of three anticyclonic eddies in the stratified Mediterranean Sea. Biogeosciences, 8: 525-538.

Vichi, M., Pinardi, N., Masina, S., 2007. A generalized model of pelagic biogeochemistry for the global ocean ecosystem. Part I: Theory. Journal of Marine Systems, 64: 89-109.

List of abbreviations and definitions

BFM	Biochemical Flux Model
ECMWF	European Centre for Medium-Range Weather Forecast
ERSEM	European Regional Seas Ecosystem Model
GETM	General Estuarine Transport Model
GRDC	Global River Data Center
LoF	Line of Frugality
MMF	Marine Modelling Framework
PFT	Plankton Functional Types
RESM	Regional Earth System Model
RfR	Redfield Ratio

List of figures

List of tables

GETTING IN TOUCH WITH THE EU

In person

All over the European Union there are hundreds of Europe Direct information centres. You can find the address of the centre nearest you at: http://europea.eu/contact

On the phone or by email

Europe Direct is a service that answers your questions about the European Union. You can contact this service:

- by freephone: 00 800 6 7 8 9 10 11 (certain operators may charge for these calls),

- at the following standard number: +32 22999696, or

- by electronic mail via: http://europa.eu/contact

FINDING INFORMATION ABOUT THE EU

Online

Information about the European Union in all the official languages of the EU is available on the Europa website at: http://europa.eu

EU publications
You can download or order free and priced EU publications from EU Bookshop at: http://bookshop.europa.eu. Multiple copies of free publications may be obtained by contacting Europe Direct or your local information centre (see http://europa.eu/contact).

KJ-NA-29142-EN-N

JRC Mission

As the science and knowledge service of the European Commission, the Joint Research Centre's mission is to support EU policies with independent evidence throughout the whole policy cycle.

EU Science Hub
ec.europa.eu/jrc

@EU_ScienceHub

EU Science Hub - Joint Research Centre

Joint Research Centre

EU Science Hub

Publications Office

doi:10.2760/797879

ISBN 978-92-79-80956-9